Convective Heat Transfer in the Boundary Layer Flow of a Maxwell Fluid Over a Flat Plate Using an Approximation Technique in the Presence of Pressure Gradient

Amber Nehan Kashif, Zainal Abdul Aziz, Faisal Salah, and K.K. Viswanathan.

***Abstract*—In this study, the effect of pressure gradient have been included for heat transfer in the boundary layer flow of Maxwell fluid over a flat plate.The solution of the problem is obtained with an application of algorithms of Adams Method (AM) and Gear Method (GM) with Homotopy Perturbation Method (HPM) as an approximation technique. This technique shows the outcomes of pressure gradient (m), Deborah number (β) and Prandtl number (Pr) in the boundary layer flow on temperature and velocity profiles, also the momentum and thermal boundary layer thickness and discussed. To obtain this objective, the momentum and energy equations of Maxwell are solved. The outcomes of HPM in the absence of relaxation time (λ) or Deborah number (β) and pressure gradient (m) (i.e. $\lambda = \beta = m = 0$) at Prandtl number $\mathrm{Pr} = 1$ are in closed relation with the numerical results having the value of η_∞ is around 5. Also it is found that the system is convergent, as a whole momentum and thermal boundary layer thicknesses becomes thinner and thinner. Importantly, some cooling effects of the Maxwell fluid over a flat plate for energy profile have been observed.**

***Index Terms*—Homotopy Perturbation Method (HPM), pressure gradient parameter, convective heat transfer, Maxwell fluid, flat plate.**

I. Introduction

THE effects of pressure gradient in the boundary layer convective heat transfer for the fluid flow has its importance. It has been discussed in Lawrence and Ran [1], Rebay and Padet [2], Fathizadeh and Rashidi [3], Aziz [4], Ishak [5] and Shagaiya and Daniel [6] for the Newtonian fluids. Chen and Chen [7] discussed Blasius boundary layer flows for two dimensional nonlinear wave propagation. Further, Chen and Weijia [8] considered pressure gradient in three-dimensional boundary layer flow for development of turbulent flow. Furthermore, Wiryanto [9] incorporated pressure gradient using Bernoulli equation and Darcy's law [10] to study for the unsteady boundary layer flow over a permeable sheet. Aziz et al. [11] determined steady state solutions of non-Newtonian fluids for magnetohydrodynamic (MHD) boundary layer flow. Boundary layers formulating boundary value problems describing nonlinear differential equations for Navior Stokes expressions have been discussed in [12], [13]. In recent years, the flows of non-Newtonian fluids have been analyzed and studied by numerous researchers. Lists of references on such flows can be found in Zierep and Fetecau [14], Fetecau and Fetecau [15], Vieru et al. [16], Hayat et al. [17] and Abbas et al. [18]. The non-Newtonian fluids are the most widely used material in many industries. The consideration of rheological constitutive equations of non-Newtonian fluids adds significantly to the complexity of the flow analysis having different parameters and, generally, the mathematicians, modelers and computer scientists encounter a wide variety of challenges in obtaining analytical, approximate and numerical solutions.

HPM is a solution method of semi-exact type. Implementation of this technique in diverse areas of nonlinear equations, fluid mechanics, integro differential equations and heat transfer have been studied by Ji-Huan [19]–[21], Cai et al. [22], Cveticanin [23], El-Shahed [24], Abbasbandy [25], Belendez et al. [26] and Esmaeilpour and Ganji [27]. Initially, Ji-Huan He in 1998 proposed the technique HPM. Later on, He and some other research workers extended and enhanced this technique for a range of nonlinear problems [28]–[34]. HPM is an efficient technique and it has been efficiently implemented to get solutions to diverse non-linear complex engineering dilemmas that cannot be worked out by analytical methods [19]–[21]. Also, the outcomes of non-Newtonian fluids has been inspected in various geometries [31], [35].

In this study,considering the convective heat transfer in the boundary layer flow of a Maxwell fluid over a flat plate in the presence of pressure gradient is explored. To obtain the solution of the problem, the two main algorithms, the Adams Method (AM) [36] and Gear Method (GM) [37], [38] have been used in [39] with an application of HPM. The outcome of pressure gradient is observed for diverse Prandtl numbers Pr and Deborah numbers β upon energy and momentum profiles and then evaluated with other solutions.

This work might be helpful in various industrial applications, circumstances associated to forced convection on the surface or in the paths of the turbo machine blades that can be abridged to an outer boundary layer problem over a wedge or a flat plate. The laminar flow system comes after the turbulent flows. Generally, turbulent flows are more

Manuscript received February 11, 2017; first revised May 23, 2017; second revised November 5, 2017.

Amber Nehan Kashif is with the Department of Mathematical Sciences, Faculty of Science, UTM and Department of Mathematical Sciences, Faculty of Science, FUUAST, Karachi, Pakistan (e-mail: ankashif@gmail.com).

Zainal Abdul Aziz is with the UTM Centre for Industrial and Applied Mathematics and Department of Mathematical Sciences, Faculty of Science, UTM (e-mail: zainalabdaziz@gmail.com).

Faisal Salah is with the Department of Mathematics, Faculty of Science, University of Kordofan,51111 El Obeid, Sudan(e-mail: faisal19999@yahoo.com).

K.K.Viswanathan is with the Kuwait College of Science and Technology, Doha Area,7th Ring Road, P.O. Box No. 27235, Safat 13133, Kuwai (e-mail: visu20@yahoo.com).

TABLE I
NOMENCLATURE

Notation	
u, v	Fluctuating Velocity Components in x and y Directions
n	Number of Approximations
T	Temperature
T_w	Wall Temperature
T_∞	Local Ambient Temperature
H	Convective Heat Transfer Coefficient
P	Pressure
L	Linear Operator
N	Non-linear Operator
AM	Adams Method
GM	Gear Method
NM	Numerical Method
HPM	Homotopy Perturbation Method
f	Dimensionless Velocity Function
m	Pressure Gradient Parameter
Pr	Prandtl Number
p	Embedding Parameter of Homotopy
$q(r)$	Analytic Function
A	General Differential Operator
B	Boundary Operator
c_p	Specific Heat
x, y	Coordinates Along and Perpendicular to The Plate
Greek Symbols	
Γ	The Boundary of The Domain Ω
ρ	The Fluid Density
η	Dimensionless Variable
δ	Boundary Layer Thickness
υ	The Kinematics Fluid Viscosity
θ	Dimensionless Temperature
ψ	Streamline Function
β	Deborah Number
λ	The Relaxation Time or Maxwell Parameter

significant than laminar flows. The study on laminar steady state forced convection can be conducted in three different ways. Firstly, the numerical technique secondly, on the bases of Blasius analysis, the differential method and thirdly, the Pohlhausens integral method [2], [40].

II. BASICS OF HPM

The fundamental concepts of this technique are given as follows:

Consider the nonlinear differential equation

$$A(u) - f(r) = 0, \quad r \in \Omega \tag{1}$$

with boundary conditions

$$B(u, \partial u/\partial n) = 0, \quad r \in \Gamma \tag{2}$$

where A is a differential operator, B is an operator, $f(r)$ is an analytic function, Γ is the domain Ω boundary. A can be divided into L linear and N nonlinear, therefore, Eq.(1) is of the form:

$$L(u) + N(u) - f(r) = 0. \tag{3}$$

By the homotopy method [40] and [2], a homotopy $\upsilon(r, P) : \Omega \times [0, 1] \to R$ is constructed, which satisfies

$$H(v, p) = (1 - p)[L(v) - L(u_o)] + p[A(v) - f(r)] = 0, \quad p \in [0, 1], \quad r \in \Omega \tag{4}$$

Or

$$H(v, p) = L(v) - L(u_o) + pL(u_o) + p[N(v) - f(r)] = 0, \tag{5}$$

where $p \in [0, 1]$ is a parameter which is embedded, u_0 is the initial approximated solution of Eq.(1), where the boundary conditions are fulfilled. Clearly, from Eq.(4 or 5) H takes the forms

$$H(v, 0) = L(v) - L(u_o) = 0, \tag{6}$$

$$H(v, 1) = A(v) - f(r) = 0, \tag{7}$$

the transformation of p from 0 to 1 is referred to $\upsilon(r, p)$ from $u_0(r)$ to $u(r)$. Topologically, this is known as deformation, besides $L(v) - L(u_0)$, $A(v) - f(r)$ are termed homotopic. In this study, the embedding parameter p as a small parameter and assumed that the solution of Eq.(4 or 5) can be written as a power series in p:

$$v = v_0 + pv_1 + p^2 v_2 + \dots \tag{8}$$

Setting $p = 1$ results in the approximate solution of Eq.(1):

$$u = \lim_{p \to 1} v = v_0 + v_1 + v_2 + \dots \tag{9}$$

The coupling of the perturbation method and the homotopy method is called the homotopy perturbation method, which eliminates limitation of the traditional perturbation methods. On the other hand, the proposed technique can take full advantage of the traditional perturbation techniques.

III. MATHEMATICAL FORMULATION

Consider the boundary layer flow over a flat plate having pressure gradient for Maxwell fluid is governed by the continuity and the momentum equations. The governing equations of continuity, motion and the energy may be written in usual notation as [6], [41], [42]:

$$\frac{\partial u}{\partial x} + \frac{\partial v}{\partial y} = 0 \tag{10}$$

$$u\frac{\partial u}{\partial x} + v\frac{\partial u}{\partial y} + \lambda\left[u^2\frac{\partial^2 u}{\partial x^2} + v^2\frac{\partial^2 u}{\partial y^2} + 2uv\frac{\partial^2 u}{\partial x \partial y}\right] = -\frac{1}{\rho}\frac{dP}{dx} + \upsilon\frac{\partial^2 u}{\partial y^2} \tag{11}$$

and

$$u\frac{\partial T}{\partial x} + v\frac{\partial T}{\partial y} = \frac{\kappa}{\rho c_p}\frac{\partial^2 T}{\partial y^2} \tag{12}$$

where u and v are the velocity components in $x-$ and $y-$ directions respectively, υ is the kinematic fluid viscosity, ρ is the fluid density, μ is the coefficient of fluid viscosity, λ is the relaxation time, T is the temperature, κ is the fluid thermal conductivity and c_p is the specific heat.

Now, the stream function $\psi(x, y)$ is introduced as:

$$u = \frac{\partial \psi}{\partial y}, \quad v = -\frac{\partial \psi}{\partial x} \tag{13}$$

For an external flow $-\frac{1}{\rho}\frac{dP}{dx}$ can be replaced by $U_\infty\frac{dU_\infty}{dx}$, where as in relations with equation (13), the equation (10) is identically satisfied and the equations (11 and 12) are reduced to the following forms:

$$\begin{aligned}&\frac{\partial\psi}{\partial y}\frac{\partial^2\psi}{\partial x\partial y}-\frac{\partial\psi}{\partial x}\frac{\partial^2\psi}{\partial y^2}+\\&\lambda\left[\left(\frac{\partial\psi}{\partial y}\right)^2\frac{\partial^3\psi}{\partial x^2\partial y}+\left(\frac{\partial\psi}{\partial x}\right)^2\frac{\partial^3\psi}{\partial y^3}-2\frac{\partial\psi}{\partial y}\frac{\partial\psi}{\partial x}\frac{\partial^3\psi}{\partial x\partial y^2}\right]\\&=U_\infty\frac{dU_\infty}{dx}+\nu\frac{\partial^3\psi}{\partial y^3}\end{aligned}\tag{14}$$

and

$$\frac{\partial\psi}{\partial y}\frac{\partial T}{\partial x}-\frac{\partial\psi}{\partial x}\frac{\partial T}{\partial y}=\frac{\kappa}{\rho c_p}\frac{\partial^2 T}{\partial y^2}\tag{15}$$

Here, we have introduced the dimension less variables η and ψ as:

$$\begin{aligned}&\eta=y\sqrt{\frac{U_\infty}{\nu x}},\quad \psi=f(\eta)\sqrt{\nu x U_\infty},\\&\theta(\eta)=\frac{T-T_\infty}{T_w-T_\infty}\quad\text{and}\\&\left\{U_\infty=Cx^m,\quad m=\frac{x}{U_\infty}\frac{dU_\infty}{dx}\right\}\end{aligned}\tag{16}$$

Based on equation (16), we have used similarity transformation to reduce the governing differential equations (14) and (15) to an ordinary non-linear differential equations (17) and (18) respectively.

$$\begin{aligned}&f'''+\frac{m+1}{2}ff''+m(1-f'^2)-\\&\frac{\beta}{2}[(m-1)(3-m)\eta f'^2f''+4m(m+1)f'^3+\\&(m+1)^2f^2f'''-2(m+1)(3m-1)ff'f'']=0,\end{aligned}\tag{17}$$

$$\theta''+\frac{\Pr(m+1)}{2}f\theta'=0.\tag{18}$$

where $\beta=\lambda U_\infty/2x$ is Deborah number [43] and $\Pr=\mu c_p/\kappa$ is the Prandtl number [18]. Using the similarity variables, we can have boundary conditions as:

$$\begin{aligned}&f(0)=0,\quad f'(0)=0,\quad f'(\eta_\infty)=1,\\&\theta(0)=1,\quad \theta(\eta_\infty)=0.\end{aligned}\tag{19}$$

IV. HPM SOLUTION

From HPM technique, equation (17) and (18) become:

$$\begin{aligned}&(1-p)(f'''-f_0''')+p(f'''+\frac{m+1}{2}ff''+\\&m(1-f'^2)-\frac{\beta}{2}[(m-1)(3-m)\eta f'^2f''+\\&4m(m+1)f'^3+(m+1)^2f^2f'''-\\&2(m+1)(3m-1)ff'f''])=0\end{aligned}\tag{20}$$

$$(1-p)(\theta''-\theta_0'')+p\left(\theta''+\frac{\Pr(m+1)}{2}f\theta'\right)=0\tag{21}$$

$$f=f_0+pf_1+p^2f_2+\ldots,\tag{22}$$

$$\theta=\theta_0+p\theta_1+p^2\theta_2+\ldots.\tag{23}$$

Assuming $f'''=0$, $\theta''=0$, and substituting f from equation (22) into equation (20) and θ from equation (23) into equation (21) after an arrangement of powers of p–terms, we have:

$$\begin{aligned}p^0:\quad&f_0'''=0,\\&f_0(0)=0,\quad f_0'(0)=0,\quad f_0'(\eta_\infty)=1,\\&\theta_0''=0,\\&\theta_0(0)=1,\quad \theta_0(\eta_\infty)=0\end{aligned}\tag{24}$$

$$\begin{aligned}p^1:\quad&f_1'''=m\left(f_0'^2-1\right)-\left(\frac{m+1}{2}\right)f_0f_0''+\\&2m\left(m+1\right)\beta f_0'^3+\\&\left(1-2m-3m^2\right)\beta f_0f_0'f_0''+\\&\frac{1}{2}\left(4m-3\eta-m^2\eta\right)\beta f_0'^2f_0''\\&f_1(0)=0,\quad f_1'(0)=0,\quad f_1'(\eta_\infty)=0,\\&\theta_1''=-\frac{\Pr(m+1)}{2}f_0\theta_0',\\&\theta_1(0)=0,\quad \theta_1(\eta_\infty)=0\end{aligned}\tag{25}$$

$$\begin{aligned}p^2:\quad&f_2'''=2mf_0'f_1'-\left(\frac{m+1}{2}\right)(f_1f_0''+f_0f_1'')+\\&6m\left(m+1\right)\beta f_0'^2f_1'+(1-2m-3m^2)\beta\\&(f_0'f_1f_0''+f_0f_0'f_1''+f_0f_1'f_0'')+\\&\left(-3+4m-m^2\right)\beta\eta\left(f_0'f_1'f_0''+\frac{1}{2}f_0'^2f_1''\right)+\\&\beta\frac{(m+1)^2}{2}\left(f_0^2f_1'''\right)\\&f_2(0)=0,\quad f_2'(0)=0,\quad f_2'(\eta_\infty)=0,\\&\theta_2''=-\frac{\Pr(m+1)}{2}(f_0\theta_1'+f_1\theta_0'),\\&\theta_2(0)=0,\quad \theta_2(\eta_\infty)=0\end{aligned}\tag{26}$$

$$\begin{aligned}p^3:\quad&f_3'''=mf_1'^2+2mf_0'f_2'-\\&\left(\frac{m+1}{2}\right)(f_2f_0''+f_1f_1''+f_0f_2'')+\\&6m(m+1)\beta\left(f_0'f_1'^2+f_0'^2f_2'\right)+\\&(1-2m-3m^2)\beta((f_2f_0'+f_1f_1'+f_0f_2')f_0''+\\&(f_1f_0'+f_0f_1')f_1''+f_0f_0'f_2'')+\\&(-3+4m-m^2)\beta\eta\\&\left(\frac{1}{2}f_1'^2f_0''+f_0'f_2f_0''+f_0'f_1f_1''+\frac{1}{2}f_0'^2f_2''\right)+\\&(1+2m+m^2)\beta\left(f_0f_1f_1'''+\frac{1}{2}f_0^2f_2'''\right),\\&f_3(0)=0,\quad f_3'(0)=0,\quad f_3'(\eta_\infty)=0,\\&\theta_3''=-\frac{\Pr(m+1)}{2}(f_0\theta_2'+f_1\theta_1'+f_2\theta_0'),\\&\theta_3(0)=0,\quad \theta_3(\eta_\infty)=0\end{aligned}\tag{27}$$

Solving equations (24)-(27):

$$f_0=\frac{1}{2\eta_\infty}(\eta^2).\tag{28}$$

$$\begin{aligned}f_1=\frac{1}{480\eta_\infty^3}(&-4\beta\eta^6+12\beta\eta^2\eta_\infty^4-2\eta^5\eta_\infty+\\&5\eta^2\eta_\infty^4+12\beta\eta^6m-36\beta\eta^2\eta_\infty^4m+\\&6\eta^5\eta_\infty m-80\eta^3\eta_\infty^3m+105\eta^2\eta_\infty^4m)\end{aligned}\tag{29}$$

$$f_2 = \frac{1}{2419200\eta_\infty^5}(812\beta^2\eta^{10} - 3024\beta^2\eta^6\eta_\infty^4 + 5012\beta^2\eta^2\eta_\infty^8 + 800\beta\eta^9\eta_\infty - 1260\beta\eta^6\eta_\infty^4 - 1008\beta\eta^5\eta_\infty^5 + 2700\beta\eta^2\eta_\infty^8 + 165\eta^8\eta_\infty^2 - 420\eta^5\eta_\infty^5 + 390\eta^2\eta_\infty^8 - \ldots) \quad (30)$$

$$f_3 = \frac{1}{83026944000\eta_\infty^7}(2067120m^5\beta^3\eta^{14} - 29150880m^4\beta^3\eta^{14} + 88679360m^3\beta^3\eta^{14} - 60281760m^2\beta^3\eta^{14} + 15444880m\beta^3\eta^{14} - 1383360\beta^3\eta^{14} + 1134000m^5\beta^2\eta_\infty\eta^{13} - 18265680m^4\beta^2\eta_\infty\eta^{13} + 61430880m^3\beta^2\eta_\infty\eta^{13} - \ldots) \quad (31)$$

$$\theta_0 = \frac{1}{\eta_\infty}(-\eta + \eta_\infty) \quad (32)$$

$$\theta_1 = \frac{1}{48\eta_\infty^2}(\eta^4 m(\mathrm{Pr}) - \eta\eta_\infty^3 m(\mathrm{Pr}) + \eta^4(\mathrm{Pr}) - \eta\eta_\infty^3(\mathrm{Pr})) \quad (33)$$

$$\theta_2 = \frac{1}{80640\eta_\infty^4}(-40\eta^7 m^2(\mathrm{Pr})^2\eta_\infty + 35\eta^4 m^2(\mathrm{Pr})^2 \eta_\infty^4 + 5\eta m^2(\mathrm{Pr})^2\eta_\infty^7 + 18\beta\eta^8 m^2(\mathrm{Pr}) - 252\beta\eta^4 m^2(\mathrm{Pr})\eta_\infty^4 + 234\beta\eta m^2(\mathrm{Pr})\eta_\infty^7 + 12\eta^7 m^2(\mathrm{Pr})\eta_\infty - 336\eta^5 m^2(\mathrm{Pr})\eta_\infty^3 + 735\eta^4 m^2(\mathrm{Pr})\eta_\infty^4 - 411\eta m^2(\mathrm{Pr})\eta_\infty^7 - 80\eta^7 m(\mathrm{Pr})^2\eta_\infty + 70\eta^4 m(\mathrm{Pr})^2\eta_\infty^4 + \ldots) \quad (34)$$

$$\theta_3 = \frac{1}{638668800\eta_\infty^6}(2772m^4(\mathrm{Pr})\beta^2\eta^{12} + 1176m^3(\mathrm{Pr})\beta^2\eta^{12} + 1232m^2(\mathrm{Pr})\beta^2\eta^{12} + 1960m(\mathrm{Pr})\beta^2\eta^{12} - 868(\mathrm{Pr})\beta^2\eta^{12} - 8640m^3(\mathrm{Pr})^2\beta\eta_\infty\eta^{11} - 14400m^2(\mathrm{Pr})^2\beta\eta_\infty\eta^{11} - 2880m(\mathrm{Pr})^2\beta\eta_\infty\eta^{11} + 2880(\mathrm{Pr})^2\beta\eta_\infty\eta^{11} + 864m^4(\mathrm{Pr})\beta\eta_\infty\eta^{11} + \ldots) \quad (35)$$

V. Results and Discussions

The value of η_∞ has its impact on the boundary layer thickness. Cebeci [40] and Bird [44] showed the results for the values of η_∞ as 8 and 5.64 for both situations velocity and energy profiles when pressure gradient $m = 0$ and Prandtl number $\mathrm{Pr} = 1$.

Results presented by Esmaeilpour and Ganji [27] for the boundary layer in the absence of pressure gradient the value of η_∞ is equal to 5 with the inclusion of velocity and temperature. In our case η_∞ have been taken as constant 5.25 for the velocity and temperature profiles.

The aim of this work is to analyze the effects of various physical parameters specially pressure gradient on the velocity and temperature distributions such as momentum and thermal boundary layer thicknesses. The validation of the present method using HPM is checked with the results obtained by Fathizadeh and Rashidi [3]. In our problem non-Newtonian (Maxwell) fluid becomes Newtonian when Deborah number is taken as zero. The reported results are the effects of m as well as β for the different values.

Figures 1 and 2 depicts the velocity profile with different values of m. These show that the velocity profile increases

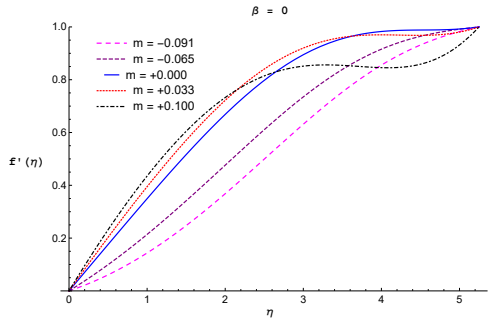

Fig. 1. Velocity profile for $f'(\eta)$ for the different values of m when $\beta = 0$ and $\eta_\infty = 5.25$.

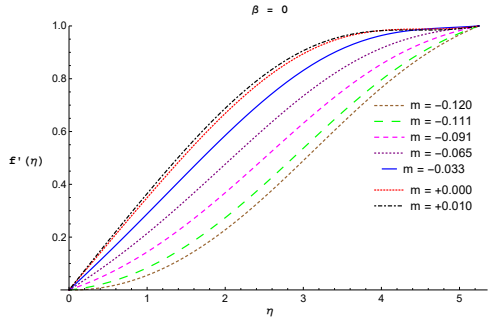

Fig. 2. Velocity profile for $f'(\eta)$ for the different values of m when $\beta = 0$ and $\eta_\infty = 5.25$.

with increasing m and consequently, the momentum boundary layer thickness becomes thicker and thicker. Here Figure 1 shows the results for higher positive values of m are not similar as in Fathizadeh and Rashidi [3] which become the case of Newtonian fluid as $\beta = 0$.

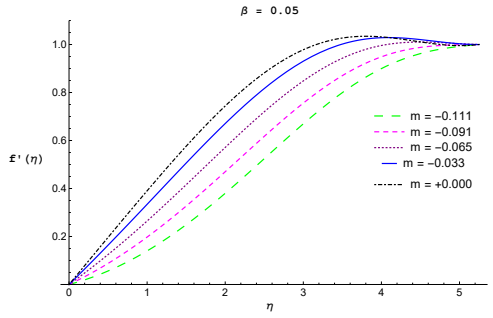

Fig. 3. Velocity profile $f'(\eta)$ for the different values of m when $\beta = 0.05$ and $\eta_\infty = 5.25$.

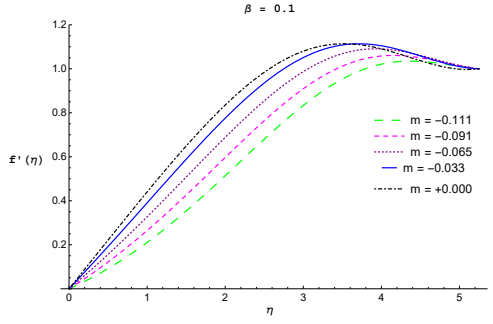

Fig. 4. Velocity profile $f'(\eta)$ for the different values of m when $\beta = 0.1$ and $\eta_\infty = 5.25$.

In Figures 3 and 4 depicts the velocity profile with

different values of m have been plotted at $\eta_\infty = 5.25$. when $\beta = 0.05$ and $\beta = 0.1$ respectively. Physically, the separation point flow is observed for lower value of m it means that the fluid is not in contact with the surface. Where as,two dimensional stagnation point flow is obtained at the higher value of m which prevents the development of the boundary layer growth. Higher value of m depicts the fluid flow is faster. Because of having a positive value of Deborah number, the effect of the flow for m is stretching towards the wall. Also show that the velocity profile increases with increasing m consequently, the momentum boundary layer thickness becomes thicker and thicker.

TABLE II
$f'(\eta)$ FOR THE VALUES OF m WHEN $\eta_\infty = 5.25$ AND $\beta = 0$

η	$f'(\eta)$ NM	HPM Results Amber et al.		
		$\beta = 0$		
		m		
		0.01	0.00	-0.12
0.0	0.000000	0.000000	0.000000	0.000000
0.2	0.066407	0.074261	0.070320	0.001390
0.4	0.132764	0.148069	0.140600	0.007590
0.6	0.198937	0.221281	0.210700	0.018600
0.8	0.264709	0.293669	0.280410	0.034430
1.0	0.329780	0.364910	0.349420	0.055050
1.2	0.393776	0.434633	0.417370	0.080450
1.4	0.456261	0.502351	0.483810	0.110550
1.6	0.516756	0.567549	0.548220	0.145220
1.8	0.574758	0.629663	0.610050	0.184300
2.0	0.629765	0.688105	0.668710	0.227510
2.2	0.681310	0.742290	0.723610	0.274500
2.4	0.728981	0.791660	0.774150	0.324810
2.6	0.772455	0.835717	0.819790	0.377910
2.8	0.811509	0.874059	0.860090	0.433150
3.0	0.846044	0.906412	0.894700	0.489810
3.2	0.876081	0.932668	0.923420	0.547090
3.4	0.901761	0.952923	0.946250	0.604150
3.6	0.923329	0.967501	0.963390	0.660160
3.8	0.941118	0.976980	0.975300	0.714310
4.0	0.955518	0.982204	0.982690	0.765850
4.2	0.966957	0.984275	0.986510	0.814120
4.4	0.975870	0.984520	0.987970	0.858630
4.6	0.982683	0.984438	0.988440	0.899020
4.8	0.987789	0.985598	0.989370	0.935080
5.0	0.991541	0.989492	0.992160	0.966720

Table II shows the results for velocity profile $f'(\eta)$ for different values of pressure gradient parameter m at Deborah number $\beta = 0$ and $\eta_\infty = 5.25$. Here it can be observed that the values of HPM results in the fourth column when $m = 0$ at $\beta = 0$ are closer to the numerical results in the second column, those published previously in Fathizadeh and Rashidi [3].

Table III are the results for velocity profile $f'(\eta)$ for the different values of pressure gradient parameter m at $\eta_\infty = 5.25$ when Deborah number $\beta = 0.05$ and $\beta = 0.1$. Figures 5 and 6 depicts the energy profile $\theta(\eta)$ with different values of m at $\eta_\infty = 5.25$ and $\beta = 0$ when $\mathrm{Pr} = 1$ and $\mathrm{Pr} = 0.5$ respectively. Because of β zero it becomes the case of Newtonian fluid. Physically, the lower and higher Deborah numbers changes their material behaviours like fluid

TABLE III
$f'(\eta)$ FOR THE VALUES OF m WHEN $\eta_\infty = 5.25$ AND $\beta = 0$

η	$f'(\eta)$ HPM Results Amber et al.			
	m			
	$\beta = 0.05$		$\beta = 0.1$	
	0.00	-0.111	0.00	-0.111
0.0	0.000000	0.000000	0.000000	0.000000
0.2	0.078605	0.019157	0.088639	0.033361
0.4	0.157153	0.042748	0.177211	0.071147
0.6	0.235491	0.070750	0.265541	0.113312
0.8	0.313366	0.103116	0.353326	0.159765
1.0	0.390418	0.139762	0.440135	0.210357
1.2	0.466186	0.180556	0.525404	0.264862
1.4	0.540111	0.225299	0.608438	0.322961
1.6	0.611543	0.273712	0.688422	0.384216
1.8	0.679761	0.325421	0.764434	0.448055
2.0	0.743989	0.379941	0.835468	0.513754
2.2	0.803424	0.436669	0.900471	0.580427
2.4	0.857273	0.494877	0.958382	0.647020
2.6	0.904788	0.553723	1.008190	0.712328
2.8	0.945322	0.612256	1.049010	0.775015
3.0	0.978377	0.669450	1.080140	0.833665
3.2	1.003660	0.724238	1.101160	0.886842
3.4	1.021160	0.775566	1.112030	0.933188
3.6	1.031160	0.822452	1.113150	0.971521
3.8	1.034350	0.864064	1.105460	1.000970
4.0	1.031780	0.899794	1.090500	1.021110
4.2	1.024950	0.929332	1.070420	1.032090
4.4	1.015710	0.952728	1.047930	1.034720
4.6	1.006210	0.970422	1.026220	1.030570
4.8	0.998748	0.983230	1.008680	1.021870
5.0	0.995522	0.992252	0.998557	1.011360

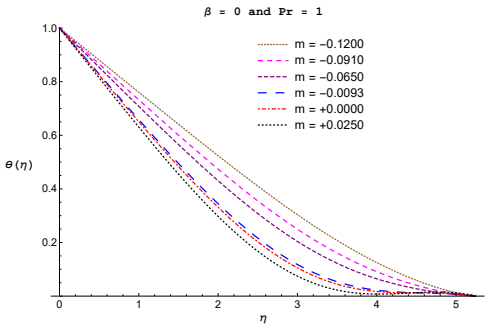

Fig. 5. Energy profile $\theta(\eta)$ for the different values of m when $\eta_\infty = 5.25$, $\beta = 0$ and $\mathrm{Pr} = 1$.

and solid, where as fluid and solid behaviour is associated with Newtonian viscous flow and non-Newtonian regime dominated by elasticity respectively. For the two different Prandtl numbers, the thermal boundary thickness decreases significantly by increasing m, consequently the thermal boundary layer thickness becomes thinner and thinner. Also it is observed that the increasing m increases the stretch of fluid temperature towards the surface and the wall.

Table IV shows the results for energy profile $\theta(\eta)$ for different values of pressure gradient parameter m at Deborah number $\beta = 0$ and $\eta_\infty = 5.25$ when $\mathrm{Pr} = 1$ and $\mathrm{Pr} = 0.5$. Here it can be observed that the values of HPM results in the fourth and seventh columns when $m = 0$ at $\beta = 0$ are

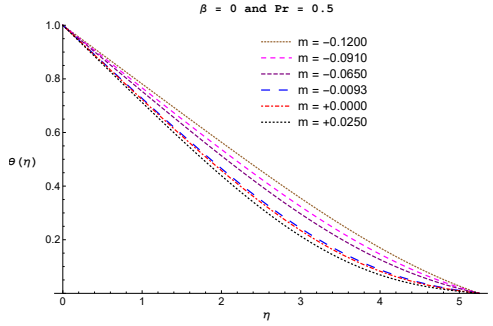

Fig. 6. Energy profile $\theta(\eta)$ for the different values of m when $\eta_\infty = 5.25$, $\beta = 0$ and $\Pr = 0.5$.

TABLE IV
$\theta(\eta)$ FOR THE VALUES OF m AT $\beta = 0$, $\eta_\infty = 5.25$ WHEN $\Pr = 1$

η	$\theta(\eta)$			
	NM	HPM		
		$\eta_\infty = 5.25$	$\beta = 0$	$\Pr = 1$
		m		
		-0.12	0.0	0.025
0.0	1.000000	1.000000	1.000000	1.000000
0.2	0.933592	0.952090	0.929672	0.925570
0.4	0.867235	0.904180	0.859394	0.851201
0.6	0.801062	0.856272	0.789295	0.777053
0.8	0.735290	0.808375	0.719590	0.703385
1.0	0.670219	0.760513	0.650575	0.630557
1.2	0.606223	0.712722	0.582625	0.559021
1.4	0.543738	0.665061	0.516189	0.489312
1.6	0.483243	0.617612	0.451775	0.422034
1.8	0.425241	0.570485	0.389943	0.357843
2.0	0.370234	0.523814	0.331281	0.297428
2.2	0.318689	0.477761	0.276389	0.241477
2.4	0.271018	0.432512	0.225850	0.190651
2.6	0.227544	0.388272	0.180201	0.145549
2.8	0.188490	0.345260	0.139901	0.106661
3.0	0.143955	0.303702	0.105293	0.074332
3.2	0.123918	0.263823	0.076572	0.048719
3.4	0.088238	0.225838	0.053745	0.029743
3.6	0.066670	0.189946	0.036603	0.017055
3.8	0.058881	0.156326	0.024693	0.010007
4.0	0.033042	0.125140	0.017307	0.007630
4.2	0.031481	0.096544	0.013480	0.008637
4.4	0.024129	0.070708	0.012021	0.011448
4.6	0.017316	0.047860	0.011556	0.014243
4.8	0.012210	0.028342	0.010630	0.015064
5.0	0.008458	0.012703	0.007835	0.011965

closer to the numerical results in the second column, those published previously in Fathizadeh and Rashidi [3].

The results for energy profile $\theta(\eta)$ for the different values of pressure gradient parameter m at Deborah number $\beta = 0$ and $\eta_\infty = 5.25$ when $\Pr = 1$ and $\Pr = 0.5$ shown in Table V. Here it can be observed that the values of HPM results in the fourth and seventh columns when $m = 0$ at $\beta = 0$ are closer to the numerical results in the second column, those published previously in Fathizadeh and Rashidi [3].

Figures 7 and 8 describes the energy profile $\theta(\eta)$ with different values of m at $\eta_\infty = 5.25$ and $\beta = 0.2$ when $\Pr = 1$ and $\Pr = 0.5$ respectively. Physically, the Prandtl number has the relative importance to thermal and momen-

TABLE V
$\theta(\eta)$ FOR THE VALUES OF m AT $\beta = 0$, $\eta_\infty = 5.25$ WHEN $\Pr = 0.5$

η	$\theta(\eta)$			
	NM	HPM		
		$\eta_\infty = 5.25$	$\beta = 0$	$\Pr = 0.5$
		m		
		-0.12	0.0	0.025
0.0	1.000000	1.000000	1.000000	1.000000
0.2	0.933592	0.956222	0.944397	0.942190
0.4	0.867235	0.912444	0.888813	0.884404
0.6	0.801062	0.868669	0.833303	0.826706
0.8	0.735290	0.824902	0.777952	0.769201
1.0	0.670219	0.781154	0.722882	0.712034
1.2	0.606223	0.737446	0.668247	0.655387
1.4	0.543738	0.693806	0.614232	0.599479
1.6	0.483243	0.650275	0.561052	0.544562
1.8	0.425241	0.606906	0.508947	0.490916
2.0	0.370234	0.563767	0.458178	0.438840
2.2	0.318689	0.520940	0.409024	0.388652
2.4	0.271018	0.478524	0.361771	0.340674
2.6	0.227544	0.436630	0.316706	0.295228
2.8	0.188490	0.395386	0.274111	0.252618
3.0	0.143955	0.354930	0.234248	0.213126
3.2	0.123918	0.315411	0.197352	0.176995
3.4	0.088238	0.276985	0.163618	0.144414
3.6	0.066670	0.239809	0.133192	0.115509
3.8	0.058881	0.204044	0.106152	0.090325
4.0	0.033042	0.169844	0.082509	0.068819
4.2	0.031481	0.137356	0.062190	0.050847
4.4	0.024129	0.106719	0.045033	0.036157
4.6	0.017316	0.078059	0.030787	0.024385
4.8	0.012210	0.051496	0.019114	0.015064
5.0	0.008458	0.027145	0.009597	0.007628

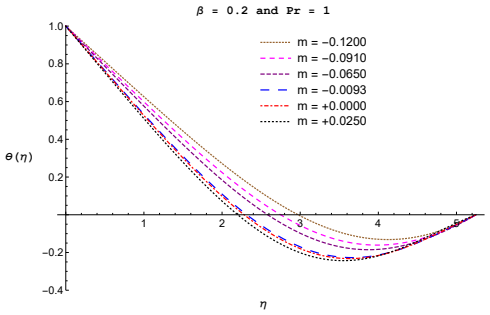

Fig. 7. Energy profile for $\theta(\eta)$ for the different values of m when $\eta_\infty = 5.25$, $\beta = 0.2$ and $\Pr = 1$.

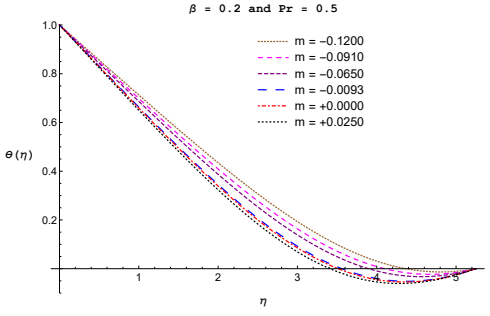

Fig. 8. Energy profile for $\theta(\eta)$ for the different values of m when $\eta_\infty = 5.25$, $\beta = 0.2$ and $\Pr = 0.5$.

tum diffusion. Lower Prandtl ($\Pr << 1$) fluids possess dominant thermal diffusivity and higher Prandtl ($\Pr >> 1$) fluids have dominant momentum diffusivity. For both Prandtl numbers, the thermal boundary thickness decreases significantly by increasing m, consequently the thermal boundary layer thickness becomes thinner and thinner. Also it is observed that the increasing m increases the stretch of fluid temperature towards the surface and the wall. The dominant momentum diffusivity leads to fast heat movement in the fluid flow or becomes good conductor .

Note that in figures above, curves of m shows negative values for $\theta(\eta)$. This is the case of cooling fluid, it is possible when the buoyancy force opposes the stretching motion of the surface, so the flow of the fluid caused by the upward motion of the surface is opposed by the free convection currents induced by buoyancy force and hence $\theta(\eta)$ decreases [45].

From the figures, it clearly shows that the positive value of β has a little impact towards cooling effect of the fluid with the Prandtl values $\Pr = 1$ and $\Pr = 0.5$.

TABLE VI
$\theta(\eta)$ FOR THE VALUES OF m AT $\beta = 0.2$, $\eta_\infty = 5.25$ WHEN $\Pr = 1$.

η	$\theta(\eta)$		
	HPM		
	$\eta_\infty = 5.25$	$\beta = 0.2$	$\Pr = 1$
	m		
	-0.12	0.0	0.025
0.0	1.000000	1.000000	1.000000
0.2	0.924856	0.904504	0.901197
0.4	0.849741	0.809085	0.802483
0.6	0.774731	0.713942	0.704081
0.8	0.699959	0.619405	0.606367
1.0	0.625617	0.525930	0.509855
1.2	0.551964	0.434101	0.415196
1.4	0.479322	0.344612	0.323169
1.6	0.408084	0.258264	0.234658
1.8	0.338708	0.175944	0.150639
2.0	0.271713	0.098600	0.072147
2.2	0.207679	0.027221	0.000251
2.4	0.147229	-0.037199	-0.06399
2.6	0.091022	-0.093704	-0.119574
2.8	0.039737	-0.141412	-0.165598
3.0	-0.005951	-0.179567	-0.201318
3.2	-0.045391	-0.207587	-0.226205
3.4	-0.07798	-0.225117	-0.240003
3.6	-0.103188	-0.232078	-0.242783
3.8	-0.120579	-0.228711	-0.234993
4.0	-0.129835	-0.21561	-0.217496
4.2	-0.130767	-0.193745	-0.19159
4.4	-0.123312	-0.164454	-0.159003
4.6	-0.107522	-0.129415	-0.121859
4.8	-0.083521	-0.090571	-0.082596
5.0	-0.051442	-0.050013	-0.043831

Table VI and Table VII shows the results for energy profile $\theta(\eta)$ for the different values of pressure gradient parameter m at Deborah number $\beta = 0.2$ and $\eta_\infty = 5.25$ when $\Pr = 1$ and $\Pr = 0.5$.

Figures 9 and 10 describes the energy profile $\theta(\eta)$ with different values of m at $\eta_\infty = 5.25$ and $\beta = -0.9$

TABLE VII
$\theta(\eta)$ FOR THE VALUES OF m AT $\beta = 0.2$, $\eta_\infty = 5.25$ WHEN $\Pr = 0.5$.

η	$\theta(\eta)$		
	$\eta_\infty = 5.25$	$\beta = 0.2$	$\Pr = 0.5$
	HPM		
	m		
	-0.12	0.0	0.025
0.0	1.000000	1.000000	1.000000
0.2	0.942404	0.931621	0.929818
0.4	0.884821	0.863276	0.859672
0.6	0.827287	0.795046	0.789656
0.8	0.769864	0.727072	0.719927
1.0	0.712640	0.659547	0.650698
1.2	0.655736	0.592720	0.582246
1.4	0.599300	0.526889	0.514897
1.6	0.543516	0.462402	0.449034
1.8	0.488599	0.399651	0.385082
2.0	0.434796	0.339065	0.323505
2.2	0.382387	0.281106	0.264799
2.4	0.331682	0.226258	0.209478
2.6	0.283017	0.175017	0.158063
2.8	0.236751	0.127877	0.111068
3.0	0.193261	0.085320	0.068987
3.2	0.152935	0.047800	0.032271
3.4	0.116160	0.015723	0.001314
3.6	0.083321	-0.010569	-0.023565
3.8	0.054780	-0.030814	-0.042150
4.0	0.030876	-0.044849	-0.054336
4.2	0.011902	-0.052625	-0.060153
4.4	-0.001898	-0.054224	-0.059779
4.6	-0.010343	-0.049869	-0.053550
4.8	-0.013323	-0.039925	-0.041968
5.0	-0.010805	-0.024908	-0.025693

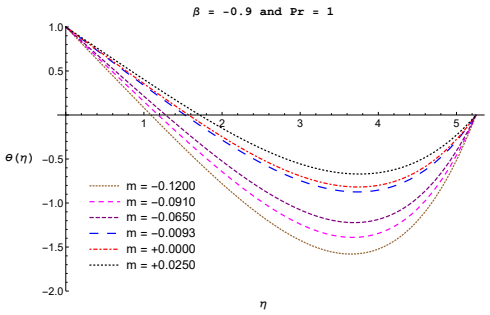

Fig. 9. $\theta(\eta)$ for the values of m when $\eta_\infty = 5.25$, $\beta = -0.9$ and $\Pr = 1$.

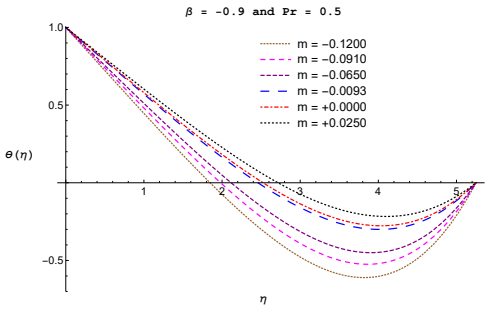

Fig. 10. Energy profile for $\theta(\eta)$ for the values of m when $\eta_\infty = 5.25$, $\beta = -0.9$ and $\Pr = 0.5$.

when $\Pr = 1$ and $\Pr = 0.5$ respectively. These show that the energy profile increasing with increasing m and consequently, the thermal boundary layer thickness becomes thicker and thicker.

Clearly, in comparison with the Figures 7 and 8 they showed that the negative value of β has it large impact towards cooling effects of the fluid with the Prandtl values $\Pr = 1$ and $\Pr = 0.5$.

TABLE VIII
$\theta(\eta)$ FOR THE VALUES OF m AT $\beta = -0.9$, $\eta_\infty = 5.25$ WHEN $\Pr = 1$.

η	$\theta(\eta)$		
	$\eta_\infty = 5.25$	$\beta = -0.9$	$\Pr = 1$
	HPM		
	m		
	-0.12	0.0	0.025
0.0	1.000000	1.000000	1.000000
0.2	0.815592	0.870404	0.880137
0.4	0.631267	0.740878	0.760345
0.6	0.447241	0.611601	0.640804
0.8	0.263882	0.482873	0.521814
1.0	0.081715	0.355112	0.403791
1.2	-0.098568	0.228856	0.287265
1.4	-0.276103	0.104761	0.172877
1.6	-0.449833	-0.016399	0.061373
1.8	-0.618503	-0.133734	-0.046395
2.0	-0.780640	-0.246236	-0.149486
2.2	-0.934535	-0.352784	-0.246864
2.4	-1.078220	-0.452141	-0.337410
2.6	-1.209470	-0.542953	-0.419929
2.8	-1.325730	-0.623749	-0.493149
3.0	-1.424150	-0.692933	-0.555726
3.2	-1.501510	-0.748781	-0.606242
3.4	-1.554230	-0.789424	-0.643200
3.6	-1.578320	-0.812838	-0.665010
3.8	-1.569350	-0.816815	-0.669974
4.0	-1.522470	-0.798943	-0.656260
4.2	-1.432350	-0.756568	-0.621859
4.4	-1.293180	-0.686748	-0.564548
4.6	-1.098660	-0.586214	-0.481825
4.8	-0.842060	-0.451305	-0.370841
5.0	-0.516202	-0.277919	-0.228323

Table VIII and Table IX are the results for energy profile $\theta(\eta)$ for the different values of pressure gradient parameter m at Deborah number $\beta = -0.9$ and $\eta_\infty = 5.25$ when $\Pr = 1$.

VI. CONCLUSION

In this study, the effect of the pressure gradient parameter has been observed for the momentum and energy equations of Maxwell's fluid over a flat plate. For this purpose, an approximation technique HPM has been used. Also, the results have been compared with the results of [3], those found to be in good agreement when pressure gradient and Deborah number considered to be zero. Furthermore, the results have been discussed for the non zero values of pressure gradient, Deborah number and Prandtl number. It is observed that the increase in pressure gradient results in increase in velocity profile whereas decrease in energy profile. Consequently for both, the momentum and thermal

TABLE IX
$\theta(\eta)$ FOR THE VALUES OF m AT $\beta = -0.9$, $\eta_\infty = 5.25$ WHEN $\Pr = 0.5$ AND $\Pr = 0.5$.

η	$\theta(\eta)$		
	$\eta_\infty = 5.25$	$\beta = -0.9$	$\Pr = 0.5$
	HPM		
	m		
	-0.12	0.0	0.025
0.0	1.000000	1.000000	1.000000
0.2	0.888879	0.915623	0.920309
0.4	0.777806	0.831282	0.840653
0.6	0.666906	0.747069	0.761121
0.8	0.556389	0.663139	0.681861
1.0	0.446555	0.579708	0.603079
1.2	0.337794	0.497052	0.525038
1.4	0.230590	0.415512	0.448058
1.6	0.125528	0.335487	0.372515
1.8	0.023293	0.257441	0.298838
2.0	-0.075319	0.181897	0.227509
2.2	-0.169406	0.109441	0.159063
2.4	-0.257945	0.040720	0.094083
2.6	-0.339792	-0.023555	0.033203
2.8	-0.413679	-0.082616	-0.022897
3.0	-0.478207	-0.135630	-0.073491
3.2	-0.531846	-0.181702	-0.117811
3.4	-0.572934	-0.219876	-0.155040
3.6	-0.599675	-0.249137	-0.184326
3.8	-0.610146	-0.268410	-0.204775
4.0	-0.602304	-0.276564	-0.215456
4.2	-0.573998	-0.272420	-0.215408
4.4	-0.522993	-0.254757	-0.203645
4.6	-0.446997	-0.222327	-0.179168
4.8	-0.343706	-0.173874	-0.140979
5.0	-0.210858	-0.108166	-0.088109

boundary layer thickness becomes thinner and thinner. The higher value of pressure gradient depicts the reduction in the viscosity of the fluid, which shows the faster behaviour of fluid flow. This behaviour of faster fluid flow is important for blood circulation in the human body. Also because of the effects of pressure gradient, the dominant momentum diffusivity leads to fast heat movement in the fluid flow which is good for conduction.

Importantly, it has been observed that the energy profile have some cooling effects for the curves of m when we take the values of Deborah number $\beta \neq 0$, for positive values it has little impact where as for negative values it has large impact of cooling for Maxwell fluid with the Prandtl values $\Pr = 1$ and $\Pr = 0.5$.

ACKNOWLEDGMENT

This research is being partially supported by the research grant under MOHE, FRGS project vote No.R.J 1300007809.4F354.

The first author (ANK) is fully supported by Federal Urdu University of Arts, Sciences & Technology (FUUAST) Karachi, Pakistan under the Faculty Development Program (FDP) of Higher Education Commission (HEC) of Pakistan. Last but not least Dr. Muhammad Arif Hussain has given a great support in this research who is affiliated to Mohammad Ali Jinnah University, Karachi, Pakistan.

REFERENCES

[1] P. S. Lawrence and B. N. Ran, "Effect of pressure gradient on MHD boundary layer over a flat plate," *Acta Mechanica*, vol. 113, pp. 1–7, 1995.

[2] M. Rebay and J. Padet, "Parametric study of unsteady forced convection with pressure gradient," *Int J of Eng Sci*, vol. 43, pp. 655–667, 2005.

[3] M. Fathizadeh and F. Rashidi, "Boundary layer convective heat transfer with pressure gradient using Homotopy Perturbation Method (HPM) over a flat plate," *Chaos, Solitons & Fractals*, vol. 42, no. 4, pp. 2413–2419, Nov. 2009.

[4] A. Aziz, "A similarity solution for laminar thermal boundary layer over a flat plate with a convective surface boundary condition," *Communications in Nonlinear Science and Numerical Simulation*, vol. 14, no. 4, pp. 1064–1068, 2009.

[5] A. Ishak, "Similarity solutions for flow and heat transfer over a permeable surface with convective boundary condition," *Applied Mathematics and Computation*, vol. 217, no. 2, pp. 837–842, 2010.

[6] Y. Shagaiya and S. Daniel, "Presence of Pressure Gradient on Laminar Boundary Layer over a Permeable Surface with Convective Boundary Condition," *American Journal of Heat and Mass Transfer*, vol. 2, no. 1, pp. 1–14, 2015.

[7] J. Chen and W. Chen, "Two-dimensional nonlinear wave dynamics in blasius boundary layer flow using combined compact difference methods," *IAENG Intl. J. Appl. Math*, vol. 41, no. 2, pp. 162–171, 2011.

[8] J. C. Chen and W. Chen, "How flow becomes turbulent," 2012.

[9] L. Wiryanto, "Unsteady waves generated by flow over a porous layer," *IAENG International Journal of Applied Mathematics*, vol. 40, no. 4, pp. 233–238, 2010.

[10] O. Polıvka and J. Mikyška, "Compositional modeling of two-phase flow in porous media using semi-implicit scheme," *IAENG Journal of Applied Mathematics*, vol. 45, no. 3, pp. 218–226, 2015.

[11] Z. A. Aziz, F. Salah, and D. L. C. Ching, "On accelerated flow for mhd generalized burgers' fluid in a porous medium and rotating frame," *IAENG International Journal of Applied Mathematics*, vol. 41, no. 3, pp. 199–205, 2011.

[12] M. Fang and B. Du, "The boundary value problems of higher order mixed type of delay differential equations." *International Journal of Applied Mathematics*, vol. 47, no. 2, 2017.

[13] M. ur Rehman, C. Vuik, and G. Segal, "Preconditioners for the steady incompressible navier-stokes problem," *International Journal of Applied Mathematics*, vol. 38, no. 4, pp. 1–10, 2008.

[14] J. Zierep and C. Fetecau, "Energetic balance for the Rayleigh Stokes problem of a Maxwell fluid," *International Journal of Engineering Science*, vol. 45, pp. 617–627, 2007.

[15] C. Fetecau and C. Fetecau, "Starting solutions for the motion of a second grade fluid due to longitudinal and torsional oscillations of a circular cylinder," *International Journal of Engineering Science*, vol. 44, no. 11-12, pp. 788–796, 2006.

[16] D. Vieru, M. Nazar, C. Fetecau, and C. Fetecau, "New exact solutions corresponding to the first problem of Stokes for Oldroyd-B fluids," *Computers & Mathematics with Applications*, vol. 55, no. 8, pp. 1644–1652, 2008.

[17] T. Hayat, Z. Abbas, M. Sajid, and S. Asghar, "The influence of thermal radiation on MHD flow of a second grade fluid," *International Journal of Heat and Mass Transfer*, vol. 50, no. 5-6, pp. 931–941, 2007.

[18] Z. Abbas, Y. Wang, T. Hayat, and M. Oberlack, "Mixed convection in the stagnation-point flow of a Maxwell fluid towards a vertical stretching surface," *Nonlinear Analysis: Real World Applications*, vol. 11, no. 4, pp. 3218–3228, Aug. 2010.

[19] H. Ji-Huan, "New interpretation of homotopy perturbation method," *International Journal of Modern Physics B*, pp. 634–638, 2006.

[20] ——, "Some asymptotic methods for strongly nonlinear equations," *International Journal of Modern Physics B*, vol. 20, no. 10, pp. 1141–1199, 2006.

[21] ——, "An elementary introduction to recently developed asymptotic methods and nanomechanics in textile engineering," *International Journal of Modern Physics B*, vol. 22, no. 21, pp. 3487–3578, 2008.

[22] X. Cai, W. Wu, and M. Li, "Approximate period solution for a kind of nonlinear oscillator by he's perturbation method," *Int. J. Nonlinear Sci. Numer. Simulation*, vol. 7, no. 1, pp. 109–112, 2006.

[23] L. Cveticanin, "Homotopy–perturbation method for pure nonlinear differential equation," *Chaos, Solitons & Fractals*, vol. 30, no. 5, pp. 1221–1230, 2006.

[24] M. El-Shahed, "Application of he's homotopy perturbation method to volterra's integro-differential equation," *International Journal of Nonlinear Sciences and Numerical Simulation*, vol. 6, no. 2, pp. 163–168, 2005.

[25] S. Abbasbandy, "Application of he's homotopy perturbation method for laplace transform," *Chaos, Solitons & Fractals*, vol. 30, no. 5, pp. 1206–1212, 2006.

[26] A. Beléndez, A. Hernandez, T. Beléndez, E. Fernández, M. Alvarez, and C. Neipp, "Application of he's homotopy perturbation method to the duffing-harmonic oscillator," *International Journal of Nonlinear Sciences and Numerical Simulation*, vol. 8, no. 1, pp. 79–88, 2007.

[27] M. Esmaeilpour and D. Ganji, "Application of he's homotopy perturbation method to boundary layer flow and convection heat transfer over a flat plate," *Physics Letters A*, vol. 372, no. 1, pp. 33–38, 2007.

[28] H. Ji-Huan, "Some Asymptotic Methods for Strongly Nonlinear Equations," *International Journal of Modern Physics B*, vol. 20, no. 10, pp. 1141–1199, 2006.

[29] ——, "Homotopy perturbation technique," *Computer methods in applied mechanics and engineering*, vol. 178, no. 3, pp. 257–262, 1999.

[30] ——, "Approximate solution of nonlinear differential equations with convolution product nonlinearities," *Computer Methods in Applied Mechanics and Engineering*, vol. 167, no. 1, pp. 69–73, 1998.

[31] M. Mahmood, M. Hossain, S. Asghar, and T. Hayat, "Application of homotopy perturbation method to deformable channel with wall suction and injection in a porous medium," *International Journal of Nonlinear Sciences and Numerical Simulation*, vol. 9, no. 2, pp. 195–206, 2008.

[32] Q. Ghori, M. Ahmed, and A. Siddiqui, "Application of homotopy perturbation method to squeezing flow of a newtonian fluid," *International Journal of Nonlinear Sciences and Numerical Simulation*, vol. 8, no. 2, pp. 179–184, 2007.

[33] A. El-Ajou, Z. Odibat, S. Momani, and A. Alawneh, "Construction of analytical solutions to fractional differential equations using homotopy analysis method," *Int. J. Appl. Math*, vol. 40, pp. 43–51, 2010.

[34] A. R. Ansari, H. Temimi, M. Kinawi, and A. M. Siddiqui, "A note on certain perturbation methods for solving the problem of fully developed flow through a porous channel," *IAENG International Journal of Applied Mathematics*, vol. 40, no. 4, pp. 224–232, 2010.

[35] A. Siddiqui, M. Ahmed, and Q. Ghori, "Couette and poiseuille flows for non-newtonian fluids," *International Journal of Nonlinear Sciences and Numerical Simulation*, vol. 7, no. 1, pp. 15–26, 2006.

[36] W. Eric Weisstein, "Adams Method." [Online]. Available: From MathWorld–A Wolfram Web Resource. http://mathworld.wolfram.com/AdamsMethod.html

[37] C. Wolfgang, "Gear Predictor-Corrector Method," 2007. [Online]. Available: Davidson University, http://webphysics.davidson.edu/Projects/SuFischer/node47.html

[38] ——, "Gear Method," 2007. [Online]. Available: University of California–San Diego, http://renaissance.ucsd.edu/chapters/chap11.pdf

[39] B. Matthew, D. Olyvia, P. Viral, S. Joel, and B. Eric Van, "Adams and Gear methods for Solving ODEs with Mathematica," 2007. [Online]. Available: https://controls.engin.umich.edu/wiki/index.php/Solving_ODEs_with_Mathematica

[40] T. Cebeci and P. Bradshaw, *Physical and Computational Aspects of Convective Heat Transfer*. New York: Springer-Verlag, 1988.

[41] K. Bhattacharyya, T. Hayat, and R. Gorla, "Heat transfer in the boundary layer flow of Maxwell fluid over a permeable shrinking sheet," *Thermal Energy and Power . . .*, vol. 2, no. 3, pp. 72–78, 2013.

[42] S. Kakaç and Y. Yener, *Convective heat transfer*. Middle East Technical University, 1980.

[43] M. Eosboee, N. Pourmahmoud, I. Mirzaie, P. M. Khameneh, S. Majidyfar, and D. Ganji, "Analytical and numerical analysis of MHD boundary layer flow of an incompressible upper-convected Maxwell fluid," *International Journal of . . .*, vol. 2, no. 12, pp. 6909–6917, 2010.

[44] R. B. Bird, W. E. Stewart, and E. N. Lightfoot, *Transport phenomena.* 2nd ed. John Wiley & Sons, 2002.

[45] J. Fan, J. Shi, and X. Xu, "Similarity solution of free convective boundary-layer behavior at a stretching surface," *Heat and Mass Transfer*, vol. 35, pp. 191–196, 1999. [Online]. Available: http://link.springer.com/10.1007/s002310050313